Available online at www.sciencedirect.com
SCIENCE DIRECT®
Journal of Solid State Chemistry 177 (2004) 4316–4324
JOURNAL OF SOLID STATE CHEMISTRY
www.elsevier.com/locate/jssc

Syntheses and structures of three new scandium selenites: $Sc_2(SeO_3)_3 \cdot H_2O$, $Sc_2(SeO_3)_3 \cdot 3H_2O$ and $CsSc_3(SeO_3)_4(HSeO_3)_2 \cdot 2H_2O$

Magnus G. Johnston, William T.A. Harrison*

Department of Chemistry, University of Aberdeen, Aberdeen AB24 3UE, Scotland, UK

Received 30 April 2004; received in revised form 13 August 2004; accepted 16 August 2004

Abstract

Three new hydrated scandium selenites have been hydrothermally synthesized as single crystals and structurally and physically characterized. $Sc_2(SeO_3)_3 \cdot H_2O$ crystallizes as a new structure type containing novel ScO_7 pentagonal bipyramidal and ScO_{6+1} capped octahedral coordination polyhedra. $Sc_2(SeO_3)_3 \cdot 3H_2O$ contains typical ScO_6 octahedra and is isostructural with its $M_2(SeO_3)_3 \cdot 3H_2O$ (M = Al, Cr, Fe, Ga) congeners. $CsSc_3(SeO_3)_4(HSeO_3)_2 \cdot 2H_2O$ contains near-regular ScO_6 octahedra and has essentially the same structure as its indium-containing analogue. All three phases contain the expected pyramidal $[SeO_3]^{2-}$ selenite groups. Crystal data: $Sc_2(SeO_3)_3 \cdot 3H_2O$, $M_r = 524.85$, trigonal, $R3c$ (No. 161), $a = 9.6481\ (5)$ Å, $c = 20.7832\ (12)$ Å, $V = 1675.45\ (16)$ Å^3, $Z = 6$, $R(F) = 0.018$, w$R(F^2) = 0.036$; $Sc_2(SeO_3)_3 \cdot H_2O$, $M_r = 488.82$, orthorhombic, $P2_12_12_1$ (No. 19), $a = 6.5913\ (6)$ Å, $b = 11.1596\ (11)$ Å, $c = 12.1368\ (11)$ Å, $V = 892.74\ (14)$ Å^3, $Z = 4$, $R(F) = 0.051$, w$R(F^2) = 0.086$; $CsSc_3(SeO_3)_4(HSeO_3)_2 \cdot 2H_2O$, $M_r = 1067.60$, orthorhombic, $Pnma$ (No. 62), $a = 16.670\ (3)$ Å, $b = 13.167\ (3)$ Å, $c = 9.575\ (2)$ Å, $V = 2101.6\ (7)$ Å^3, $Z = 4$, $R(F) = 0.035$, w$R(F^2) = 0.070$.

Keywords: Hydrothermal synthesis; Crystal structure; Scandium; Selenium

1. Introduction

The crystal structures of inorganic solids containing the $[Se^{IV}O_3]^{2-}$ selenite ion are of interest due to the asymmetric coordination polyhedron adopted by this species [1]. This effect can be rationalized [2] in terms of the stereochemically active (nonbonded) lone pair of electrons possessed by Se^{IV}, which invariably leads to a pyramidal shape for the $[SeO_3]^{2-}$ species. It has been suggested [3] that this may lead to a tendency for selenites to crystallize in noncentrosymmetric structures with consequent interesting physical properties, such as nonlinear optical second harmonic generation (SHG). In addition, crystal structures containing selenite moieties must accommodate the space-filling requirements of the Se lone pair electrons which can lead to open-channel structures [4,5].

Here, we report the hydrothermal syntheses, single-crystal structures and some characterization data for the three new hydrated scandium selenites $Sc_2(SeO_3)_3 \cdot H_2O$, $Sc_2(SeO_3)_3 \cdot 3H_2O$ and $CsSc_3(SeO_3)_4(HSeO_3)_2 \cdot 2H_2O$. Previous studies of the scandium/selenium/oxygen system have described the single crystal structures of the scandium selenites $Sc(HSeO_3)_3$ [6] and $Sc_2(SeO_3)_3$ [7], and the scandium selenates $(NH_4)_3Sc(SeO_4)_3$ [8], $Sc(SeO_4)(HSeO_4) \cdot 2H_2O$ [9] and $Sc_2(SeO_4)_3 \cdot 5H_2O$ [10].

*Corresponding author. Fax: +44-1224-272-921.
E-mail address: w.harrison@abdn.ac.uk (W.T.A. Harrison).

0022-4596/$ - see front matter © 2004 Elsevier Inc. All rights reserved.
doi:10.1016/j.jssc.2004.08.026

2. Experimental

2.1. Synthesis

$Sc_2(SeO_3)_3 \cdot 3H_2O$ was prepared by a hydrothermal reaction, as follows: 0.277 g (2 mmol) Sc_2O_3 and 12 mL of 0.5 M "H_2SeO_3" (dissolved SeO_2) solution were sealed in an 18-mL capacity, teflon-lined, stainless steel autoclave (pre-oven pH $\sim$ 1.5). The autoclave was heated to 180 °C for 3 days, followed by cooling to room temperature over a few hours. The solid product, consisting of 0.905 g of transparent cubes of $Sc_2(SeO_3)_3 \cdot 3H_2O$ (85% yield based on Sc), was recovered from the supernatant liquor by vacuum filtration and washing with water and acetone.

To prepare $Sc_2(SeO_3)_3 \cdot H_2O$, 0.277 g (2 mmol) Sc_2O_3, 0.390 g (2 mmol) $CsNO_3$ and 15 mL of 0.5 M H_2SeO_3 solution were sealed in a 23-mL capacity, teflon-lined, steel autoclave (pre-oven pH $\sim$ 1.5). The autoclave was heated to 165 °C for 25 days, followed by cooling to room temperature over a few hours. The solid product, consisting of 0.802 g of transparent needles and rods of $Sc_2(SeO_3)_3 \cdot H_2O$ (80% yield based on Sc) was recovered by vacuum filtration and washing with water and acetone.

If the first reaction is repeated (i.e. $T = 180$ °C, heating time = 3 days) with the amount of $CsNO_3$ used increased to 0.780 g (4 mmol), transparent bars of $CsSc_3(SeO_3)_4(HSeO_3)_2 \cdot 2H_2O$ begin to appear in the product mixture. Interestingly, the majority phase is $Sc_2(SeO_3)_3 \cdot 3H_2O$ (in a visually estimated 5:1 ratio) and no $Sc_2(SeO_3)_3 \cdot H_2O$ is produced. These reactions are reproducible.

2.2. Structure determinations

In each case, a suitable single crystal [$Sc_2(SeO_3)_3 \cdot 3H_2O$, colorless block, $\sim 0.12 \times 0.12 \times 0.12$ mm; $Sc_2(SeO_3)_3 \cdot H_2O$, colorless needle, $0.28 \times 0.03 \times 0.02$ mm; $CsSc_3(SeO_3)_4(HSeO_3)_2 \cdot 2H_2O$, colorless bar, $0.31 \times 0.11 \times 0.06$ mm] was mounted on a thin glass fibre with cyanoacrylate adhesive and intensity data were collected on a Bruker SMART1000 CCD diffractometer ($T = 20$ °C, Mo $K\alpha$ radiation, $\lambda = 0.71073$ Å) with the aid of the SMART and SAINT packages [11]. Empirical "multi-scan" absorption corrections were applied with SADABS [12] on the basis of multiply-measured and symmetry-equivalent reflections, with resulting correction-factor ranges of 0.351–0.404, 0.113–0.875, and 0.106–0.507, for $Sc_2(SeO_3)_3 \cdot 3H_2O$, $Sc_2(SeO_3)_3 \cdot H_2O$, and $CsSc_3(SeO_3)_4(HSeO_3)_2 \cdot 2H_2O$, respectively.

For each structure, most of the atoms were located by direct methods [13]. The remaining nonhydrogen atoms were routinely located during the full matrix least-squares refinement stage (program SHELXL-97) [14]. For $Sc_2(SeO_3)_3 \cdot 3H_2O$, the systematic absences indicated the noncentrosymmetric space group $R3c$ (No. 161) or centrosymmetric $R\bar{3}c$ (No. 167). The former was chosen on the basis of previous studies of isostructural phases [15–18]. For the chosen crystal of $Sc_2(SeO_3)_3 \cdot 3H_2O$, the Flack absolute structure parameter [19] refined to 0.555 (9) indicating merohedral (racemic) twinning. The water H atoms were located in a difference map and refined by riding on their attached O atom. A PLATON [20] analysis of the refined structure did not indicate any "missed" symmetry. For $Sc_2(SeO_3)_3 \cdot H_2O$, the systematic absences indicated space group $P2_12_12_1$ (No. 19). The refined value of the Flack parameter, 0.52 (2), indicated merohedral twinning. Due to the weak scattering from the needle-like crystal, the thermal parameters for the oxygen atoms were refined isotropically. No H atoms could be definitively located although they must be attached to O10, the water molecule O atom. For $CsSc_3(SeO_3)_4(HSeO_3)_2 \cdot 2H_2O$ the systematic absences indicated either the noncentrosymmetric space group $Pna2_1$ (No. 33), or, with appropriate axis transformations (as presented in Table 1), the centrosymmetric space group $Pnma$ (No. 62). The latter option was chosen on the basis of the previous study of the isostructural indium phase [21] and the refinement proceeded satisfactorily. The cesium cation is disordered over adjacent sites, and various refinement schemes were tried to most effectively model this feature (vide infra). The H atoms were located from difference maps or by geometrical placement and refined by riding on their carrier O atoms. The basic crystallographic data and details of data collection/refinement are summarized in Table 1. Supplementary data in cif format are available from the authors or from the inorganic crystal structure database (ICSD), maintained by the Fachinformationzentrum (FIZ), Karlsruhe, Germany [deposition numbers: CSD-391277 for $Sc_2(SeO_3)_3 \cdot 3H_2O$, CSD-391279 for $Sc_2(SeO_3)_3 \cdot H_2O$, and CSD-391278 for $CsSc_3(SeO_3)_4(HSeO_3)_2 \cdot 2H_2O$].

2.3. Physical characterization

Thermogravimetric analyses of well-powdered samples of $Sc_2(SeO_3)_3 \cdot H_2O$ and $Sc_2(SeO_3)_3 \cdot 3H_2O$ were carried out on a Mettler Toledo TGA/SDTA instrument from room temperature to 900 °C, with a heating rate of 1 °C/min under air. Room temperature infrared spectroscopic data for $Sc_2(SeO_3)_3 \cdot H_2O$ and $Sc_2(SeO_3)_3 \cdot 3H_2O$ were collected on a Nicolet Nexus 670/870 FT-IR Spectrometer. In both cases around 5 mg of sample was ground with 200 mg of oven-dried KBr, and pressed into a thin pellet. There was insufficient amount of pure $CsSc_3(SeO_3)_4(HSeO_3)_2 \cdot 2H_2O$ to perform similar measurements.

Table 1
Crystallographic parameters for $Sc_2(SeO_3)_3 \cdot H_2O$, $Sc_2(SeO_3)_3 \cdot 3H_2O$ and $CsSc_3(SeO_3)_4(HSeO_3)_2 \cdot 2H_2O$

	$Sc_2(SeO_3)_3 \cdot 3H_2O$	$Sc_2(SeO_3)_3 \cdot H_2O$	$CsSc_3(SeO_3)_4(HSeO_3)_2 \cdot 2H_2O$
Formula weight	524.85	488.82	1067.60
Crystal system	Trigonal	Orthorhombic	Orthorhombic
a (Å)	9.6481 (5)	6.5913 (6)	16.670 (3)
b (Å)	9.6481 (5)	11.1596 (11)	13.167 (3)
c (Å)	20.7832 (12)	12.1368 (11)	9.5749 (19)
α (°)	90	90	90
β (° C)	90	90	90
γ (°)	120	90	90
V (Å^3)	1675.45 (16)	892.74 (14)	2101.6 (7)
Z	6	4	4
Space group	*R3c* (No. 161)	$P2_12_12_1$ (No. 19)	*Pnma* (No.62)
ρ_{calc} (g/cm^3)	3.121	3.637	3.374
μ (cm^{-1})	110.46	137.9	131.3
$2\theta_{max}$ (°)	65	60	65
Reflections measured	5321	7636	21028
Unique reflections	1349	2597	3954
R_{int}	0.027	0.094	0.074
Parameters	53	87	160
Min./max $\Delta\rho$ (e/Å^3)	−0.41/+0.45	−1.19/+1.20	−1.41/+1.51
$R(F)$	0.018	0.051	0.035
w$R(F^2)$	0.036	0.086	0.070

3. Results

3.1. Crystal structure of $Sc_2(SeO_3)_3 \cdot 3H_2O$

The atomic positional and displacement parameters are listed in Table 2 and selected bond distance and bond angle data are presented in Table 3. This noncentrosymmetric, polar, phase contains seven non-hydrogen atoms (1 Se, 2 Sc, 4 O) in the asymmetric unit and is isostructural with its $M_2(SeO_3)_3 \cdot 3H_2O$ (M = Al, [15], Fe [16], Ga [17], Cr [18]) analogues. Both scandium atoms lie on special positions with three-fold symmetry and are coordinated by six O atoms [mean d(Sc1–O) = 2.075 (2) Å, bond valence sum (BVS) based on the Brown formalism [22] for Sc1 = 3.25 (expected 3.00); mean d(Sc2–O) = 2.101 (2) Å, BVS(Sc2) = 2.98] in fairly regular octahedral geometry.

The $Se1O_3$ group adopts its normal [1] trigonal pyramidal geometry [d_{av} (Se1–O)= 1.685 (2) Å, BVS(Se1) = 4.23], with the O–Se–O bond angles ranging from 95.51 (10) to 102.20 (12)°, with the unobserved Se^{IV} lone pair assumed to occupy the fourth tetrahedral vertex. Interestingly, the maximum difference peak of 0.45 e/Å^3 for $Sc_2(SeO_3)_3 \cdot 3H_2O$ is 0.81 Å from Se1 in roughly the position expected for its lone pair electrons. Atoms O1, O2 and O3 take part in Sc–O–Se bridges [θ_{av} (Sc–O–Se) = 130.2 (2)°; BVS(O1) = 1.88; BVS(O2) = 2.03; BVS(O3) = 2.00, expected 2.00], whilst O4, bonded only to Sc2, is the oxygen atom of the water molecule [BVS(O4) = 0.42 when neglecting H atoms].

Table 2
Atomic positional/displacement parameters for $Sc_2(SeO_3)_3 \cdot 3H_2O$

Atom	x	y	z	U_{eq}
Sc1	0	0	0.15861 (3)	0.01228 (13)
Sc2	0	0	0.39277 (3)	0.01561 (14)
Se1	0.09665 (3)	0.27964 (3)	0.277131 (13)	0.01642 (5)
O1	0.2638 (3)	0.4616 (2)	0.26980 (10)	0.0334 (5)
O2	0.1401 (3)	0.1951 (3)	0.21595 (11)	0.0378 (6)
O3	0.1422 (2)	0.2003 (3)	0.34034 (10)	0.0327 (5)
O4	0.1926 (3)	0.0515 (3)	0.45912 (10)	0.0403 (6)
H1[a]	0.2034	0.0746	0.5038	0.048
H2[a]	0.2886	0.0580	0.4458	0.048

[a]H atoms refined by riding on O4 with $U_{iso}(H) = 1.2U_{eq}(O4)$.

The basic building unit of $Sc_2(SeO_3)_3 \cdot 3H_2O$ consists of an $Sc1O_6$ octahedron linked to an $Sc2O_3(OH_2)_3$ octahedron via three equivalent bridging selenite groups as Sc1–O2–Se1–O3–Sc3 bridges (Fig. 1). These [$Sc_2(SeO_3)_3 \cdot 3H_2O$] units stack with their Sc1···Sc2 axes aligned along the polar [001] direction as shown in Fig. 2, and in turn, are crosslinked in the (001) plane by the Se1–O1–Sc1 links to similar [$Sc_2(SeO_3)_3 \cdot 3H_2O$] units displaced by +1/6 in the [001] direction. The hydrogen bonding scheme (see Table 3 for symmetry codes) stabilizes this polyhedral arrangement, with three equivalent O4–H1···O1^{vii} bonds linking adjacent

Table 3
Selected bond lengths (Å) and angles (°) for $Sc_2(SeO_3)_3 \cdot 3H_2O$

Sc1–O2	2.060 (2)	Sc1–O2^{i}	2.060 (2)
Sc1–O2^{ii}	2.060 (2)	Sc1–O1^{iii}	2.0896 (19)
Sc1–O1^{iv}	2.0896 (19)	Sc1–O1^{v}	2.0896 (19)
Sc2–O3^{i}	2.038 (2)	Sc2–O3^{ii}	2.038 (2)
Sc2–O3	2.038 (2)	Sc2–O4	2.163 (2)
Sc2–O4^{i}	2.163 (2)	Sc2–O4^{ii}	2.163 (2)
Se1–O2	1.6735 (19)	Se1–O3	1.6856 (19)
Se1–O1	1.6958 (18)		
Se1–O1–Sc1^{vi}	128.28 (11)	Se1–O2–Sc1	132.45 (12)
Se1–O3–Sc2	130.00 (12)		

D–H···A	*d*(D–H)	*d*(H···A)	*d*(D···A)	< (D–H···A)
O4–H1···O1^{vii}	0.95	2.15	3.087(3)	173
O4–H2···O1^{viii}	0.94	2.09	3.003(3)	163

Symmetry transformations used to generate equivalent atoms: (i) $-y$, $x-y$, z; (ii) $y-x$, $-x$, z; (iii) $2/3-y$, $1/3-x$, $z-1/6$; (iv) $-1/3-x+y$, $y-2/3$, $z-1/6$; (v) $x-1/3$, $x-y+1/3$, $z-1/6$; (vi) $1/3-y$, $2/3-x$, $z+1/6$; (vii) $2/3-y$, $1/3+x-y$, $1/3+z$; (viii) $1/3-x+y$, $2/3+y$, $1/6+z$.

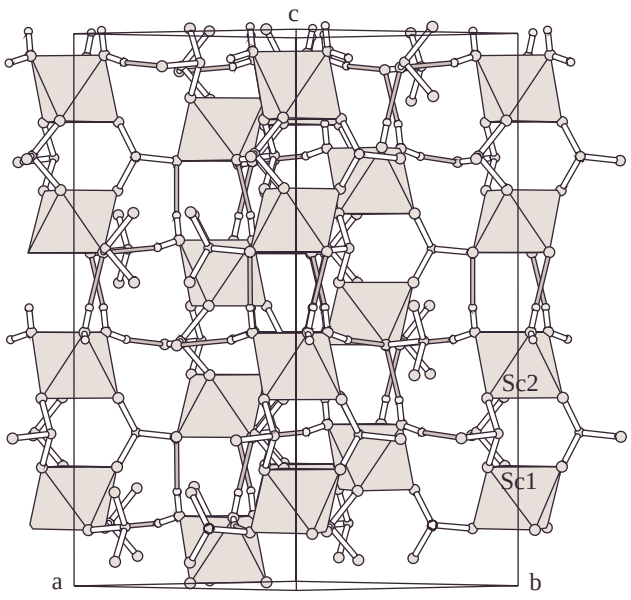

Fig. 2. Unit cell packing of $Sc_2(SeO_3)_3 \cdot H_2O$ projected onto (110) with the scandium–oxygen octahedra represented by polyhedral figures and H···O interactions by thin, shaded, lines.

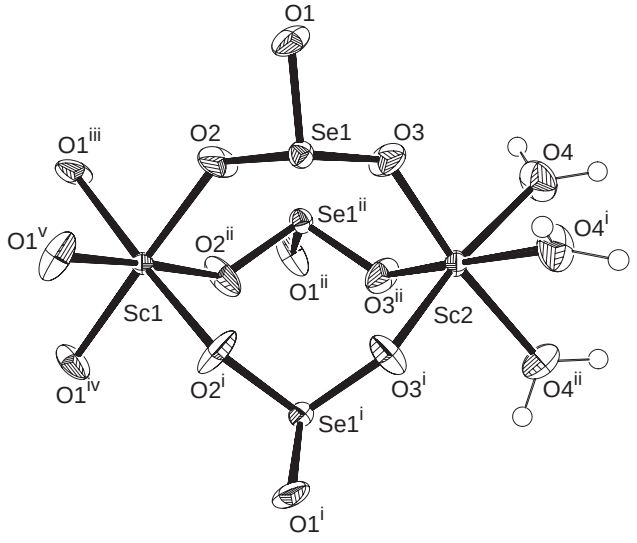

Fig. 1. Fragment of $Sc_2(SeO_3)_3 \cdot 3H_2O$ (50% displacement ellipsoids, small spheres of arbitrary radius for the H atoms) showing the linking of the $Sc1O_6$ and $Sc2O_3(H_2O)_3$ octahedra by three selenite moieties, thus forming a "lantern" motif. Symmetry codes as in Table 3.

$[Sc_2(SeO_3)_3 \cdot 3H_2O]$ units in the [001] direction, and the O4–H2···O1^{viii} bond crosslinking to a similar moiety in an adjacent [001] stack.

In $Fe_2(SeO_3)_3 \cdot 3H_2O$ [16], a similar hydrogen bonding scheme is observed with a slightly shorter O4···O1^{vii} separation (using our atom labelling scheme) of 3.058 Å compared to that observed here [*d*(O4···O1^{vii}) = 3.087 (3) Å]. Overall, $Sc_2(SeO_3)_3 \cdot 3H_2O$ fits quite well into the rhombohedral $M_2(SeO_3)_3 \cdot 3H_2O$ (M = Al, Fe, Cr, Ga) family, although it is worth noting that Sc^{3+} (ionic radius = 0.745 Å) [23] is significantly the largest trivalent cation to be accommodated into this structure type. This is reflected in the $Sc_2(SeO_3)_3 \cdot 3H_2O$ unit-cell volume of 1675.45 (16) Å^3, compared to the cell volume of 1539.9 Å^3 for $Fe_2(SeO_3)_3 \cdot 3H_2O$ containing the next-largest cation, Fe^{3+} (r = 0.645 Å), an increase of about 9%.

3.2. Crystal structure of $Sc_2(SeO_3)_3 \cdot H_2O$

The atomic positional and displacement parameters are listed in Table 4 and selected bond distance and angle data are presented in Table 5. This new structure type contains 15 nonhydrogen atoms (3 Se, 2 Sc, 10 O) in the asymmetric unit (Fig. 3).

Both the scandium cations in $Sc_2(SeO_3)_3 \cdot H_2O$ have very unusual coordination environments: Sc1 has six nearest-neighbor [*d*(Sc1–O) < 2.17 Å] oxygen atoms in a heavily distorted octahedral arrangement. The O2^{iv}–Sc1–O5 and O2^{iv}–Sc1–O6^{iii} *cis* bond angles of 122.0 (3)° and 68.3 (3)° are particularly obtuse and acute, respectively (see Table 5 for full symmetry information) and the angular variance [24], σ^2_{oct}, of the 12 *cis* angles has the large value of 144.7. The (nominal) *trans* O–Sc1–O bond angles range from 154.1 (3)° to 179.6 (3)°. There is a seventh O atom associated with Sc1, with *d*(Sc1–O1^{iv}) = 2.605 (7) Å. This distance is far longer than the expected Sc–O bond length of 2.13 Å based on the ionic radius sum [23] for octahedral Sc^{3+} and O^{2-}, but is shorter than typical nonbonded contacts of 3 Å or more. When this distant O atom is included in the

Table 4
Atomic positional/displacement parameters for $Sc_2(SeO_3)_3 \cdot H_2O$

Atom	x	y	z	U_{eq}
Sc1	0.7883 (3)	0.54618 (14)	−0.01210 (13)	0.0108 (4)
Sc2	0.2771 (3)	0.40458 (13)	−0.07351 (14)	0.0108 (4)
Se1	0.29612 (16)	0.19991 (7)	0.15046 (8)	0.0109 (2)
Se2	0.30578 (17)	0.65624 (7)	0.04316 (8)	0.0125 (2)
Se3	0.82716 (16)	0.37012 (8)	0.22012 (8)	0.0127 (2)
O1	0.0851 (11)	0.1223 (6)	0.1116 (6)	0.0234 (17)[a]
O2	0.4463 (10)	0.1137 (5)	0.0660 (5)	0.0123 (14)[a]
O3	0.2764 (10)	0.3326 (5)	0.0841 (5)	0.0156 (15)[a]
O4	0.2721 (10)	0.7725 (5)	−0.0425 (5)	0.0162 (15)[a]
O5	0.4687 (10)	0.5650 (6)	−0.0280 (5)	0.0136 (16)[a]
O6	0.1092 (10)	0.5612 (5)	0.0118 (5)	0.0130 (15)[a]
O7	0.7481 (11)	0.4848 (5)	0.1430 (6)	0.0248 (17)[a]
O8	0.6683 (10)	0.3895 (5)	0.3276 (5)	0.0139 (14)[a]
O9	0.7188 (11)	0.2515 (5)	0.1587 (5)	0.0175 (15)[a]
O10[b]	0.1964 (12)	0.5058 (5)	−0.2238 (5)	0.0211 (15)[a]

[a] U_{iso}.
[b] The H atoms attached to the O10 water molecule were not located.

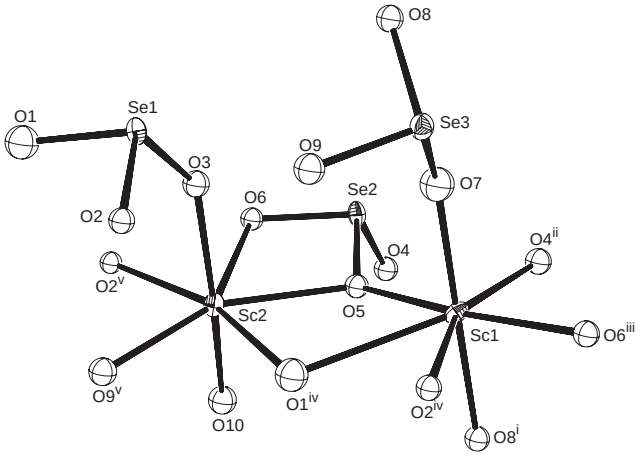

Fig. 3. Fragment of $Sc_2(SeO_3)_3 \cdot H_2O$ (50% displacement ellipsoids for Sc and Se; 50% isotropic spheres for O) showing the $Sc1O_{6+1}$ (including the long Se1–O1^{iv} bond which essentially bisects the O5···O2^{iv} octahedral edge) and $Sc2O_7$ polyhedra and pyramidal selenite moieties. The H atoms attached to O10 (the water molecule) were not found. Note the edge sharing between the $Sc1O_{6+1} + Sc2O_7$ groupings. Symmetry codes as in Table 5.

Table 5
Selected bond lengths (Å) and angles (°) for $Sc_2(SeO_3)_3 \cdot H_2O$

Sc1–O7	2.020 (7)	Sc1–O8^{i}	2.093 (6)
Sc1–O5	2.125 (7)	Sc1–O4^{ii}	2.132 (6)
Sc1–O6^{iii}	2.142 (7)	Sc1–O2^{iv}	2.168 (6)
Sc1–O1^{iv}	2.605 (7)	Sc2–O9^{v}	2.062 (6)
Sc2–O3	2.074 (6)	Sc2–O1^{iv}	2.104 (7)
Sc2–O2^{v}	2.191 (7)	Sc2–O10	2.211 (6)
Sc2–O5	2.259 (7)	Sc2–O6	2.313 (6)
Se1–O3	1.691 (6)	Se1–O1	1.705 (7)
Se1–O2	1.719 (6)	Se2–O4	1.677 (6)
Se2–O5	1.714 (7)	Se2–O6	1.717 (7)
Se3–O7	1.669 (6)	Se3–O9	1.679 (6)
Se3–O8	1.687 (6)		
Se1–O1–Sc2^{v}	157.0 (4)	Se1–O1–Sc1^{v}	94.3 (3)
Sc2^{v}–O1–Sc1^{v}	106.9 (3)	Se1–O2–Sc1^{v}	111.3 (3)
Se1–O2–Sc2^{iv}	126.9 (3)	Sc1^{v}–O2–Sc2^{iv}	114.5 (3)
Se1–O3–Sc2	141.1 (3)	Se2–O4–Sc1^{vi}	122.3 (3)
Se2–O5–Sc1	129.3 (4)	Se2–O5–Sc2	104.1 (3)
Sc1–O5–Sc2	119.9 (3)	Se2–O6–Sc1^{vii}	145.5 (4)
Se2–O6–Sc2	101.8 (3)	Sc1^{vii}–O6–Sc2	110.7 (3)
Se3–O7–Sc1	137.9 (4)	Se3–O8–Sc1^{viii}	132.7 (4)
Se3–O9–Sc2^{iv}	144.1 (4)		

Symmetry transformations used to generate equivalent atoms: (i) $3/2 - x$, $1 - y$, $z - 1/2$; (ii) $x + 1/2$, $3/2 - y$, $-z$; (iii) $x + 1$, y, z; (iv) $x + 1/2$, $1/2 - y$, $-z$; (v) $x - 1/2$, $1/2 - y$, $-z$; (vi) $x - 1/2$, $3/2 - y$, $-z$; (vii) $x - 1$, y, z; (viii) $3/2 - x$, $1 - y$, $z + 1/2$.

coordination environment of Sc1 a mono-capped octahedral or severely distorted pentagonal bipyramidal arrangement is seen (Fig. 3). This capping occurs through an edge (O5···O2^{iv}), effectively bisecting the O5–Sc1–O2 bond angle (for the Sc1, O5, O2^{iv}, and O1^{iv} grouping: root-mean-square deviation from the best least-squares plane = 0.033 Å). The bond valence sum (BVS) for Sc1 for the six near-neighbor O atoms is 2.96, rising to 3.09 if the seventh, more distant O atom is included.

Sc2 is surrounded by seven O atom neighbors [d(Sc2–O) < 2.32 Å] in a slightly distorted pentagonal bipyramidal arrangement (Fig. 3). The atoms O1^{iv}, O2^{v}, O5, O6 and O9^{v} reside at the equatorial (eq) positions with (O–Sc2–O)$_{eq}$ bond angles ranging from 63.7 (3)° to 87.0 (3)° [sum of (O–Sc2–O)$_{eq}$ angles = 359.9°; for the six atoms, r.m.s. deviation from the best least-squares plane = 0.069 Å], whilst O3 and O10 (the latter being the O atom of the water molecule), occupy the axial positions [θ(O10–Sc2–O3) = 163.4 (3)°]. Based on these seven contributors, the BVS of 2.99 for Sc2 is in excellent agreement with the expected 3.00. The longest Sc2–O bond [d(Sc2–O6) = 2.313 (6) Å] contributes a significant 0.29 v.u. to the overall BVS, supporting the validity of regarding this geometry as fundamentally pentagonal bipyramidal. This is, to the best of our knowledge, the first example of such a coordination polyhedron for Sc^{3+} in extended inorganic structures.

The three crystallographically distinct selenite groups show their expected [1] trigonal pyramidal coordinations [d_{av}(Se1–O) = 1.705 (6) Å, BVS(Se1) = 4.01; d_{av}(Se2–O) = 1.703 (7) Å, BVS(Se2) = 4.04; d_{av}(Se3–O) = 1.678 (7) Å, BVS(Se3) = 4.32], although the $[Se1O_3]^{2-}$ and $[Se2O_3]^{2-}$ groups are considerably more distorted than $[Se3O_3]^{2-}$. The O–Se–O bond angles range from 91.2 (3)° to 104.5 (3)° for Se1, and from 89.7 (3)° to 103.9 (3)° for Se2 (a range of around 14°), whilst those for Se3 are clustered in a much smaller range between 98.2 (3)° and 102.9 (3)° (range < 5°). These bond angle variations can be rationalized in terms

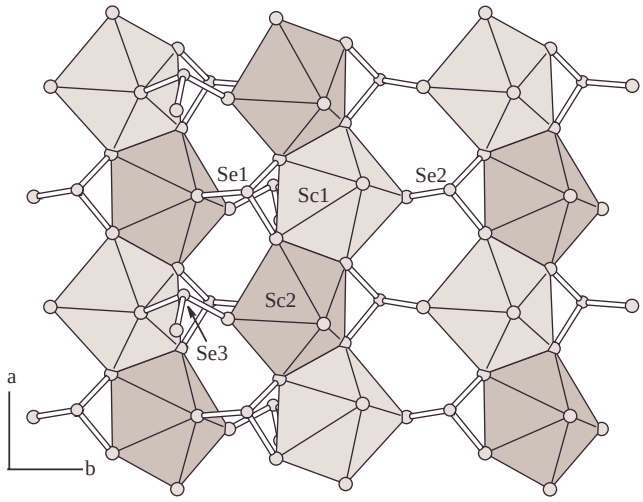

Fig. 4. Projection onto (001) of a polyhedral layer in $Sc_2(SeO_3)_3 \cdot H_2O$ (see text) with the scandium/oxygen groups represented by solid figures. Shading key: $Sc1O_7$ polyhedra very light shading, $Sc2O_7$ polyhedra light shading.

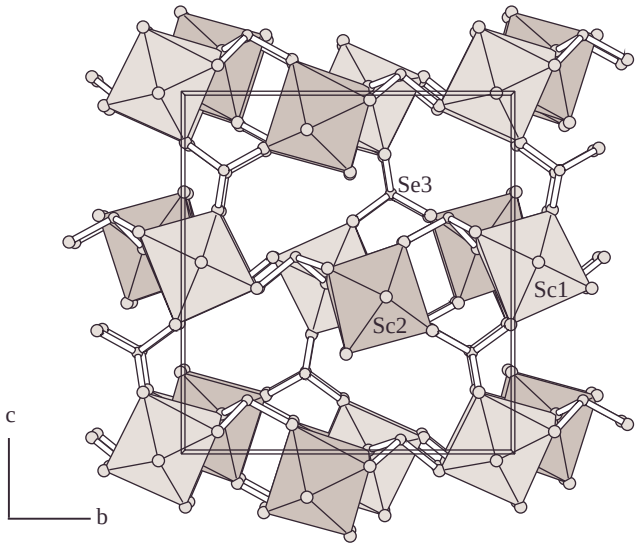

Fig. 5. Unit cell packing in $Sc_2(SeO_3)_3 \cdot H_2O$ projected onto (100). Shading scheme as in Fig. 4.

of the differing structural roles the selenite groups have in the three-dimensional structure (see below). O1, O2, O5 and O6 are tri-coordinate to two Sc and one Se, whilst O3, O4, O7, O8 and O9 form vertex-sharing Sc–O–Se bridges ($\theta_{av} = 135.7^\circ$). Bond valence sums for these nine framework O atoms range from 1.90 to 2.11. O10 is the water molecule, with BVS(O10) = 0.38. Although the H atoms associated with O10 were not located, they may be involved in O–H···O hydrogen bonds, as several O10···O contacts in the range 2.74–3.00 Å are present in the structure.

The polyhedral connectivity in $Sc_2(SeO_3)_3 \cdot H_2O$ can be described as follows: chains of $Sc1O_{6+1}$ and $Sc2O_7$ groups, alternately sharing edges (via O1 and O5, and O2 and O6), propagate along [100]. The relatively acute edge-sharing Sc1–O–Sc2 bond angles [range 106.9 (3)° to 119.9 (3)°] correlate well with the very compressed O–Sc–O bond angles [range 61.3 (2)° to 68.3 (2)°] involved in the edge sharing connectivity. The Sc/O chains are cross-linked in the [010] direction by the $Se1O_3$ and $Se2O_3$ groups via edge- and vertex-sharing Sc–O–Se bridges, forming infinite (001) sheets (Fig. 4). The edge-sharing interactions between Se2 and Sc2 (via O5 and O6), and Se1 and Sc2 (via O1 and O2) account for the extremely compressed O–Se1–O and O–Se2–O bond angles described above. The Se1 and Se2 lone pairs point roughly normal to the (001) sheets. The $Se3O_3$ groups link adjacent sheets in the [001] direction via Se3–O7–Sc1, Se3–O8–Sc1 and Se3–O9–Sc2 bridges [mean θ(Se3–O–Sc) = 138.4(5)°]. When viewed down [100] (Fig. 5) it can be seen how the lone pair electrons of the $Se1O_3$ and $Se2O_3$ groups, as well as the O atom of the water molecule, are orientated into the regions between the Sc/Se1/Se2/O sheets.

Table 6
Atomic positional/displacement parameters for $CsSc_3(SeO_3)_4(HSeO_3)_2 \cdot 2H_2O$

Atom	x	y	z	U_{eq}
Cs1[a]	0.78594 (9)	3/4	−0.0073 (2)	0.0474 (4)
Cs2[a]	0.7483 (6)	3/4	−0.0838 (10)	0.087 (3)
Sc1	0.62475 (4)	0.49991 (5)	0.17761 (7)	0.01087 (13)
Sc2	0.55853 (6)	3/4	0.55503 (10)	0.0139 (2)
Se1	0.41785 (2)	0.49108 (3)	0.16653 (4)	0.01485 (9)
Se2	0.71351 (2)	0.59596 (3)	0.48604 (4)	0.01475 (9)
Se3	0.57103 (3)	1/4	0.15506 (5)	0.01340 (12)
Se4	0.57260 (3)	3/4	0.17709 (5)	0.01465 (12)
O1	0.35292 (18)	0.5760 (2)	0.2504 (3)	0.0252 (7)
H1[b]	0.3172	0.5452	0.3033	0.030
O2	0.42206 (17)	0.5520 (2)	0.0140 (3)	0.0178 (6)
O3	0.50368 (16)	0.5261 (2)	0.2463 (3)	0.0189 (6)
O4	0.75838 (16)	0.5102 (2)	0.5943 (3)	0.0177 (6)
O5	0.66420 (18)	0.5154 (2)	0.3814 (3)	0.0232 (7)
O6	0.64038 (18)	0.6367 (2)	0.5954 (3)	0.0233 (7)
O7	0.4838 (2)	1/4	0.2449 (4)	0.0218 (9)
O8	0.62059 (18)	0.34714 (19)	0.2315 (3)	0.0222 (7)
O9	0.5926 (3)	3/4	0.3499 (4)	0.0254 (10)
O10	0.62986 (18)	0.65252 (19)	0.1220 (3)	0.0190 (6)
O11	0.46912 (19)	0.6350 (2)	0.4968 (3)	0.0296 (7)
H2[c]	0.4673	0.6100	0.4145	0.035
H3[c]	0.4770	0.5883	0.5710	0.035

[a]Site occupancies: Cs1 0.738 (6), Cs2 0.269(7).
[b]H1 refined by riding on O1 with $U_{iso}(H) = 1.2U_{eq}(O1)$.
[c]H2 and H3 refined by riding on O11 with $U_{iso}(H) = 1.2U_{eq}(O11)$.

3.3. Crystal structure of $CsSc_3(SeO_3)_4(HSeO_3)_2 \cdot 2H_2O$

The atomic positional and displacement parameters are listed in Table 6 and selected bond distance and bond angle data are presented in Table 7. This phase contains 19 nonhydrogen atoms (two disordered Cs, 4 Se, 2 Sc, 11 O) in the asymmetric unit (Fig. 6). Atoms

Table 7
Selected bond lengths (Å) and angles (°) for $CsSc_3(SeO_3)_4(HSeO_3)_2 \cdot 2H_2O$

Sc1–O5	2.069 (3)	Sc1–O8	2.078 (3)
Sc1–O10	2.080 (3)	Sc1–O2^{i}	2.107 (3)
Sc1–O4^{ii}	2.109 (3)	Sc1–O3	2.151 (3)
Sc2–O7^{iii}	2.041 (4)	Sc2–O9	2.044 (4)
Sc2–O6	2.058 (3)	Sc2–O6^{iv}	2.058 (3)
Sc2–O11	2.196 (3)	Sc2–O11^{iv}	2.196 (3)
Se1–O2	1.668 (3)	Se1–O3	1.686 (3)
Se1–O1	1.751 (3)	Se2–O5	1.675 (3)
Se2–O6	1.694 (3)	Se2–O4	1.705 (3)
Se3–O7	1.689 (4)	Se3–O8	1.689 (3)
Se3–O8^{v}	1.689 (3)	Se4–O10	1.684 (3)
Se4–O10^{iv}	1.684 (3)	Se4–O9	1.688 (4)
Se1–O2–Sc1^{i}	126.21 (15)	Se1–O3–Sc1	127.88 (14)
Se2–O4–Sc1^{vi}	132.59 (15)	Se2–O5–Sc1	141.54 (17)
Se2–O6–Sc2	126.20 (15)	Se3–O7–Sc2^{iii}	140.9 (2)
Se3–O8–Sc1	129.92 (15)	Se4–O9–Sc2	152.5 (3)
Se4–O10–Sc1	129.26 (15)		

D–H…A	d(D–H)	d(H…A)	d(D…A)	<(D–H…A)
O1–H1…O4^{iii}	0.88	1.76	2.635 (4)	176
O11–H2…O3	0.85	2.04	2.853 (4)	158
O11–H3…O3^{iii}	0.95	2.33	3.280 (4)	180

Symmetry transformations used to generate equivalent atoms: (i) $1-x, 1-y, -z$; (ii) $3/2-x, 1-y, z-1/2$; (iii) $1-x, 1-y, 1-z$; (iv) $x, 3/2-y, z$; (v) $x, 1/2-y, z$; (vi) $3/2-x, 1-y, z+1/2$.

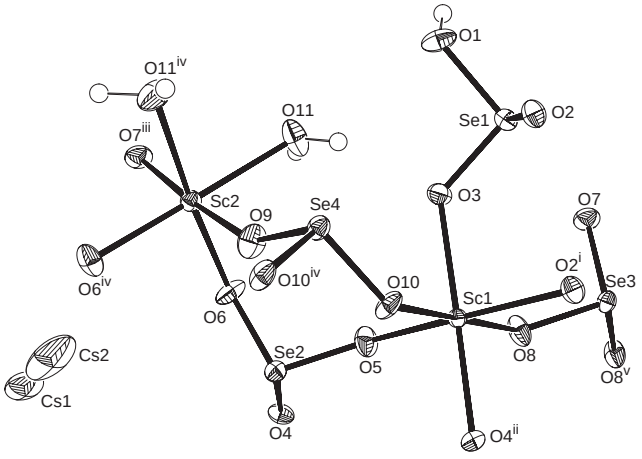

Fig. 6. Fragment of $CsSc_3(SeO_3)_4(HSeO_3)_2 \cdot 2H_2O$ (50% displacement ellipsoids, small spheres of arbitrary radius for the H atoms). Cs–O bonds omitted for clarity. Symmetry codes as in Table 7.

Cs1, Cs2, Se3, Se4, Sc2 and O7 all have site symmetry *m*, whilst the other atoms are situated on general positions. $CsSc_3(SeO_3)_4(HSeO_3)_2 \cdot 2H_2O$ is isostructural with $CsIn_3(SeO_3)_4(HSeO_3)_2 \cdot 2H_2O$ [21] although the cesium atom locations appear to be slightly different in the two phases.

Both Sc1 and Sc2 are octahedrally coordinated by six O atoms [d_{av}(Sc1–O) = 2.099 (3) Å, BVS(Sc1) = 3.06; d_{av}(Sc2–O) = 2.098 (3) Å, BVS(Sc2) = 3.09]. Two of the O atoms (2 × O11) coordinating Sc2 are part of water molecules and are in *cis* positions. The *cis* O–Sc–O bond angles range from 82.66 (11) to 97.62 (12)° (spread = 15°) in $Sc1O_6$, and from 86.82 (12) to 93.06 (11)° (spread = 6.3°) in $Sc2O_4(OH_2)_2$. The *trans* O–Sc1–O angles lie between 166.07 (12)° and 179.38 (12)° (spread = 13.3°), whilst those for the more regular Sc2 group are clustered in the very narrow range between 175.60 (12) and 175.87 (18)°.

The lengthened, protonated, Se1–O1H [d(Se1–O1) = 1.751 (3) Å] bond in $CsSc_3(SeO_3)_4(HSeO_3)_2 \cdot 2H_2O$ is typical for the hydrogen selenite group. The other three selenite groups display their usual pyramidal geometry [d_{av}(Se2–O) = 1.691 (3) Å; d_{av}(Se3–O) = 1.692 (3) Å; d_{av}(Se4–O) = 1.686 (3) Å] with O–Se–O bond angles for these three groupings in the range between 98.41 (19) and 102.54 (15)° (spread = 4.1°). The protonated selenite group is slightly more distorted with the O–Se1–O bond angles varying between 96.91 (13) and 103.26 (13)° (spread = 6.4°). Bond valence sums for the four Se(IV) species yield values of 4.04 (Se1), 4.12 (Se2), 4.13 (Se3) and 4.20 (Se4).

The Cs^+ cations show positional disorder over two or more adjacent sites, with refined site occupation factors (s.o.f) of 0.738 (6) for Cs1 and 0.269 (7) for Cs2 [d(Cs1⋯Cs2) = 0.965 (11) Å; unrestrained occupancy sum = 1.007 (7)]. However, the displacement ellipsoid for Cs2 is distinctly anisotropic which could indicate further, unresolved positional disorder. In the indium phase [21] the Cs^+ cation was modeled to be disordered over three adjacent sites.

The polyhedral connectivity in $CsSc_3(SeO_3)_4(HSeO_3)_2 \cdot 2H_2O$, which only involves Sc–O–Se bonds, can be described as follows. Pairs of adjacent $Sc1O_6$ octahedra are bridged by the $Se1O_3H$ units via O3 and O2. In turn, these moieties are linked to similar neighbors in the *b* direction by the Se3 and Se4-centered selenite groups. The $Sc2O_4(H_2O)_2$ polyhedra crosslink the [010] double chains by way of the Sc2–O7–Se3 and Sc2–O9–Se4 bonds, hence forming an infinite anionic sheet of stoichiometry $[Sc_3(SeO_3)_4(HSeO_3)_2]^-$. The lone pair electrons of the Se3 species appear to be orientated into small cavities formed by the four ring chains within the sheet. The sheets stack in the *a* direction, with adjacent sheets linked through the $Se2O_3$ units. The [100] connectivity between the sheets is reinforced by Se1–O1–H1⋯O4^{iii} hydrogen bonding (see Table 7). When viewed down [001] (Fig. 7) it can be seen how the three-dimensional Sc/Se/O framework surrounds [001] channels which encapsulate the disordered Cs^+ cations. The inter-polyhedral Se–O–Sc bond angles range from 126.29 (15) to 152.6 (3)°.

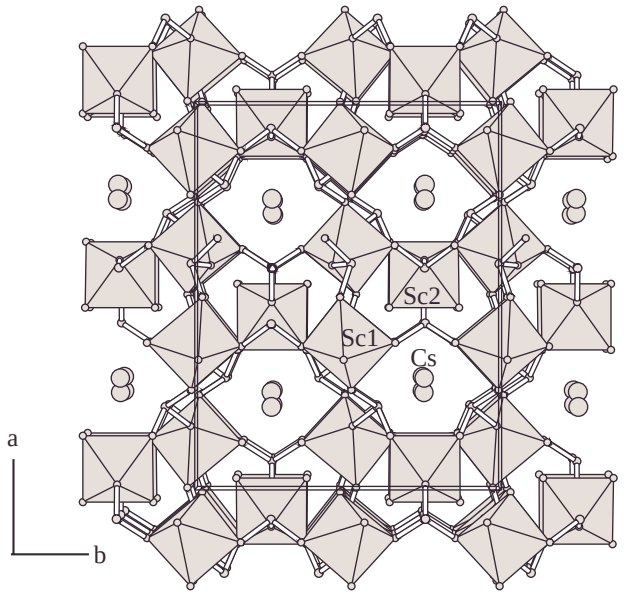

Fig. 7. Projection onto (001) of the unit cell packing in $CsSc_3(SeO_3)_4(HSeO_3)_2 \cdot 2H_2O$ showing the [001] channels occupied by Cs^+ cations.

3.4. Thermal analysis

TGA for $Sc_2(SeO_3)_3 \cdot 3H_2O$ showed two well-defined weight losses: the first occurs between 185 and 240 °C (−8.4%), with a second following between about 380 and 900 °C (−58.1%; total −66.5%). A reasonable decomposition scheme is as follows: $Sc_2(SeO_3)_3 \cdot 3H_2O \rightarrow$ " $Sc_2(SeO_3)_3$" $+ 3H_2O$ (gas) (calculated weight loss = 10.3%) $\rightarrow Sc_2O_3 + 3SeO_2$ (gas) (calculated total weight loss = 63.4%). Powder XRD on the end product indicated the presence of Sc_2O_3. In the isostructural chromium and iron-containing $M_2(SeO_3)_3 \cdot 3H_2O$ phases, the water loss stages are complete by 420 and 300 °C respectively, with decomposition to Cr_2O_3 and Fe_2O_3 complete by 550 and 600 °C, respectively. Thus, the scandium phase loses water more easily, but the loss of SeO_2 occurs more slowly, over a broad temperature range. Such sluggish thermal decompositions are not unusual for selenites [1]. Powder XRD on samples of $Cr_2(SeO_3)_3 \cdot 3H_2O$ heated to 400 °C indicated that the intermediate phase was amorphous, whilst the end product was found to be Cr_2O_3.

TGA for $Sc_2(SeO_3)_3 \cdot H_2O$ showed two losses: −3.7% between 320 and 500 °C and −62.8% (total = −66.5%) between about 540 and 850 °C, suggesting a decomposition scheme according to $Sc_2(SeO_3)_3 \cdot H_2O \rightarrow$ "$Sc_2(SeO_3)_3$" $+H_2O$ (gas) (calculated weight loss = 3.6%) $\rightarrow Sc_2O_3 + 3SeO_2$ (gas) (calculated total weight loss = 63.4%). Powder XRD on the end product indicated the presence of Sc_2O_3.

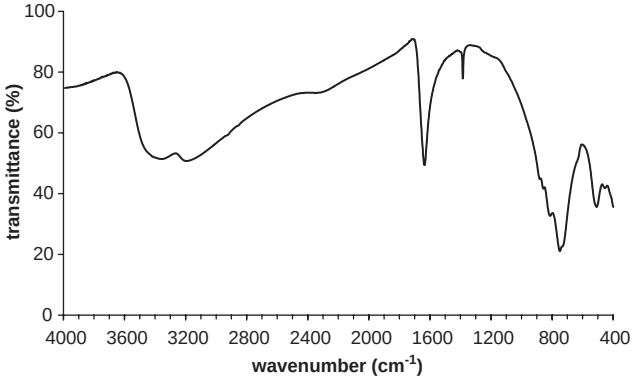

Fig. 8. IR spectrum of $Sc_2(SeO_3)_3 \cdot 3H_2O$.

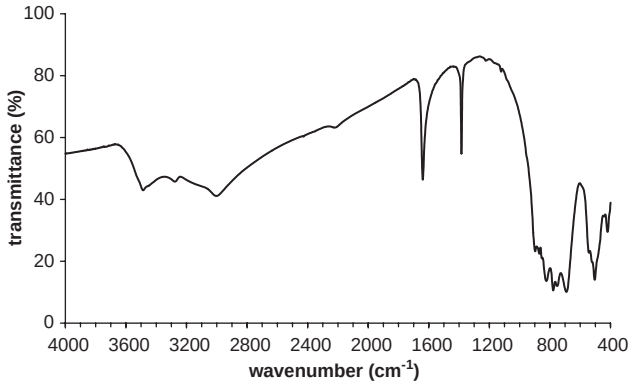

Fig. 9. IR spectrum of $Sc_2(SeO_3)_3 \cdot H_2O$.

3.5. Infrared spectroscopy

The IR spectra of $Sc_2(SeO_3)_3 \cdot 3H_2O$ and $Sc_2(SeO_3)_3 \cdot H_2O$ are shown in Figs. 8 and 9, respectively. Both show a number of peaks in the 3600–2900 cm^{-1} range, confirming the presence of hydrogen bonded water in both samples, whilst the relatively sharp and intense peaks at 1640 cm^{-1} can be assigned to H–O–H bending modes. The array of overlapping, strong peaks between 1000 and 400 cm^{-1} arises from partially-resolved framework Se–O, O–Se–O and Sc–O vibrations [25].

4. Discussion

Three new scandium selenite hydrates, $Sc_2(SeO_3)_3 \cdot 3H_2O$, $Sc_2(SeO_3)_3 \cdot H_2O$, and $CsSc_3(SeO_3)_4(HSeO_3)_2 \cdot 2H_2O$, have been prepared at moderate temperatures (165–180 °C), once again demonstrating the utility of the hydrothermal method to prepare single crystals of new metal selenites [1]. These phases complement the previously characterized scandium selenites, $Sc(HSeO_3)_3$ [6] and $Sc_2(SeO_3)_3$ [7], which contain fairly regular ScO_6

octahedra. $Sc_2(SeO_3)_3 \cdot 3H_2O$ and $CsSc_3(SeO_3)_4(HSeO_3)_2 \cdot 2H_2O$ possess isostructural analogues as described above. $Sc_2(SeO_3)_3 \cdot H_2O$ crystallizes as a completely new structure type, distinct from $Fe_2(SeO_3)_3 \cdot H_2O$ [26], which contains FeO_6 and $FeO_5(H_2O)$ octahedra. We could find no other trivalent metal selenite hydrates of formula $M_2(SeO_3)_3 \cdot H_2O$.

In this study, the concentration of $CsNO_3$ in the reactant mixture seems to have a crucial (and curious) role in determining which phase(s) results from the reaction. The effect is apparently not related to the reaction pH, since the initial pH is always around 1.5 irrespective of the $CsNO_3$ concentration. If the $CsNO_3$ is omitted from the reaction mixture, single crystals of $Sc_2(SeO_3)_3 \cdot 3H_2O$ are the only product in high yield. With the addition of 2 mmol of $CsNO_3$, only $Sc_2(SeO_3)_3 \cdot H_2O$ is produced, yet when the quantity of $CsNO_3$ is increased to 4 mmol the majority phase reverts to the tri-hydrate and a small amount of $CsSc_3(SeO_3)_4(HSeO_3)_2 \cdot 2H_2O$ appears in the product mixture. It is unclear why the mono-hydrate can only be synthesized at a specific cesium nitrate concentration, however, Wildner [27] has reported a similar (and unexplained) effect, whereby the *C*-centered monoclinic modification of $CoSeO_3$ could only be synthesized in the presence of Rb^+ cations which are not incorporated into the resulting structure.

From a structural perspective, the compounds differ in the way their common polyhedral building units are assembled. $Sc_2(SeO_3)_3 \cdot 3H_2O$ contains ScO_6 octahedra bridged in a "lantern" motif by three SeO_3 pyramids, and only vertex sharing between the polyhedra. $Sc_2(SeO_3)_3 \cdot H_2O$, which contains unusual ScO_7 groups is the only phase of the three to show Sc–O–Sc bonds (via polyhedral edge-sharing) and also ScO_7/SeO_3 edge sharing. $CsSc_3(SeO_3)_4(HSeO_3)_2 \cdot 2H_2O$ only shows vertex sharing between the ScO_6 and SeO_3 moieties, but in this case, only two SeO_3 groups bridge nearby ScO_6 octahedra. This inter-polyhedral flexibility suggests that there may be more scandium selenites to be discovered, if the hydrothermal conditions required to prepare them can be discovered.

Acknowledgments

We thank Brian Paterson for assistance with the TGA measurements and the University of Aberdeen for financial support (MGJ). We thank an anonymous referee for helpful advice on the TGA measurements.

References

[1] V.P. Verma, Thermochim. Acta 327 (1999) 63.
[2] J.K. Burdett, Molecular Shapes, Wiley-Interscience, New York, 1980.
[3] K.M. Ok, P.S. Halasyamani, Chem. Mater. 14 (2002) 2360.
[4] W.T.A. Harrison, Z. Zhang, J. Solid State Chem. 133 (1997) 572.
[5] M.G. Johnston, W.T.A. Harrison, Acta Crystallogr. C 58 (2002) i33.
[6] J. Valkonen, M. Leskelae, Acta Crystallogr. B 34 (1978) 1323.
[7] J. Valkonen, Acta Crystallogr. B 34 (1978) 1957.
[8] J. Valkonen, L. Niinisto, Acta Crystallogr. B 34 (1978) 266.
[9] J. Valkonen, Acta Crystallogr. B 34 (1978) 3064.
[10] J. Valkonen, L. Niinisto, B. Eriksson, L.O. Larsson, U. Skoglund, Acta Chem. Scand. 29 (1975) 866.
[11] SMART and SAINT software for area-detector diffractometers, Bruker AXS Inc., Madison, WI, USA.
[12] G.M. Sheldrick, Program SADABS for absorption corrections for area-detector data, University of Göttingen, Germany.
[13] G.M. Sheldrick, Program SHELXS-97 for direct-methods structure solution, University of Göttingen, Germany.
[14] G.M. Sheldrick, Program SHELXL-97, University of Göttingen, Germany.
[15] W.T.A. Harrison, G.D. Stucky, R.E. Morris, A.K. Cheetham, Acta Crystallogr. C 48 (1992) 1365.
[16] G. Giester, F. Pertlik, J. Alloys Comp. 210 (1994) 125.
[17] R.K. Rastsvetaeva, V.I. Andrianov, A.N. Volodina, Dokl. Akad. Nauk SSSR 291 (1986) 352.
[18] W.T.A. Harrison, G.D. Stucky, A.K. Cheetham, Eur. J. Solid State Inorg. Chem. 30 (1993) 347.
[19] H.D. Flack, Acta Crystallogr. A 39 (1983) 876.
[20] A.L. Spek, J. Appl. Crystallogr. 36 (2003) 7.
[21] R.K. Rastsvetaeva, V.I. Andrianov, A.N. Volodina, Dokl. Akad. Nauk SSSR 277 (1984) 871.
[22] I.D. Brown, J. Appl. Crystallogr. 29 (1996) 479.
[23] R.D. Shannon, Acta Crystallogr. A 32 (1976) 751.
[24] K. Robinson, G.V. Gibbs, P.H. Ribbe, Science (Washington, DC) 172 (1971) 567.
[25] K. Nakamoto, Infrared and Raman Spectra of Inorganic and Coordination Compounds, Wiley-Interscience, New York, 1997.
[26] G. Giester, J. Solid State Chem. 103 (1993) 451.
[27] M. Wildner, J. Solid State Chem. 120 (1995) 182.